Building and Environment 282 (2025) 113259

Contents lists available at ScienceDirect

Building and Environment

journal homepage: www.elsevier.com/locate/buildenv

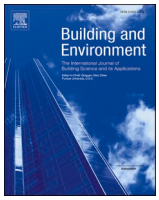

User evaluations of fabric shades with sun in the field of view: Glare model performance and implications for EN14501 Classification

Caroline Karmann [a,b,*], Jan Wienold [a], Julieta Alejandra Yamin Garreton [c], Ayelén María Villalba [c], Andrea Elvira Pattini [c], Marilyne Andersen [c]

[a] Laboratory of Integrated Performance in Design (LIPID), École Polytechnique Fédérale de Lausanne (EPFL), Switzerland
[b] Laboratory of Architecture and Intelligent Living (AIL), Karlsruhe Institute of Technology (KIT), Germany
[c] Institute of Environment, Habitat and Energy (INAHE), National Scientific and Technical Research Council (CONICET), Mendoza, Argentina

ARTICLE INFO

Keywords:
Discomfort glare
Fabric shadings
User assessment
Daylight
Glare prediction
Visual comfort

ABSTRACT

Discomfort glare from daylight is common in workspaces, where daylight and luminance contrast between light source and background can be excessive. Fabric shadings can mitigate glare, but their light transmission properties remain difficult to characterize. This study evaluates the recommended glare classes in EN17037+A1:2022 and EN14501:2021 by analyzing data from two laboratory studies (Switzerland and Argentina) and a simulation study. The experiments involved 55 participants across 191 sessions, testing four fabrics with a low openness factor (OF<7%). Using the Osterhaus-Bailey subjective scale for glare perception, we found comfortable glare conditions (i.e., not disturbing nor intolerable) for 87-96% participants with class 3 and class 1 fabrics under the tested scenarios. However, we also found that the existing tabular classification tends to overestimate glare for fabrics with normal-normal transmittance $\tau_{v,\ n\text{-}n}$ larger than 0.03 are involved, as well for fabrics with lighter colors that have higher diffuse transmittances ($\tau_{v,\ n\text{-}dif}$ >0.03). Common glare metrics (DGP, CGI, UGP) showed strong correlations with subjective responses on the Osterhaus-Bailey scale (Spearman $\rho > 0.5$). DGP showed the highest correlation ($\rho = 0.57$) with a disturbing glare threshold of 0.43, indicating that the standard threshold of 0.40 slightly overestimates glare for shading fabrics when the sun is in the field of view. DGP_{mod} did not perform significantly different than DGP. ROC analysis based on binary classification confirmed acceptable to excellent discrimination ability for DGP, CGI and UGP. Based on these findings and annual simulations, we recommend adjustments to the glare classification in EN14501:2021.

1. Introduction

The International Commission on Illumination (CIE) defines glare as the "condition of vision in which there is discomfort or a reduction in the ability to see details or objects, caused by an unsuitable distribution or range of luminance, or by extreme luminance contrasts" [1]. In this definition, we distinguish the notion of *discomfort glare* (i.e. generating an annoyance) from *disability glare* (i.e. generating an actual reduction in the ability to see objects). Discomfort glare from daylight is common in workspaces and represents a major source of disturbance for building occupants [2] that can affect one's perceived level of productivity [3]. It is the focus of the present study.

Discomfort glare can be modelled using two variables: the amount of light reaching the eye and the luminance contrast [4,5]. Some metrics are solely based on the former, as is the case for instance for: vertical illuminance at the eye level (E_v), average luminance, Simplified Daylight Glare Probability (DGPs) [6]. Others are dominated by the latter, such as for: Daylight Glare Index (DGI) [7,8], Unified Glare Probability (UGP) [9] (based on the Unified Glare Rating (UGR) [10]), and CIE Glare Index (CGI) [10,11]. Some further metrics are based on both effects: these hybrid metrics would include Predicted Glare Sensation Vote (PGSV) [12] and Daylight Glare Probability (DGP) [13]. Looking at the effectiveness of discomfort glare metrics, DGP was identified to be the most robust and reliable one available to date [4,14] and was adopted for daylight glare prediction in the European standard EN17037, EN14501 and EN12464-1 [15].

While external shading devices have the potential to achieve higher energy savings compared to interior mounted systems, the resulting visual comfort conditions will always mainly depend, for given external conditions, glazing properties and interior layout, on the material

* Corresponding author.
E-mail address: caroline.karmann@hefr.ch (C. Karmann).

https://doi.org/10.1016/j.buildenv.2025.113259
Received 7 March 2025; Received in revised form 5 May 2025; Accepted 3 June 2025
Available online 15 June 2025

properties of the shading. Among them, fabrics are interesting elements because they are usually familiar to building occupants, are rather inexpensive compared to other shading systems, and depending on their properties, may allow a view to the outside even when closed. Although fabric shadings appear simple at first glance, their anisotropic behavior is complex and require the measurement of their Bidirectional Scattering Distribution Function (BTDF) to fully characterize them. "Simpler" properties, such as normal-hemispherical transmittance ($\tau_{v,\ n\text{-}h}$), normal-normal visual transmittance ($\tau_{v,\ n\text{-}n}$), normal-diffuse visual transmittance ($\tau_{v,\ n\text{-}dif}$), cut-off angle and openness factor (OF), are thus typically used in standards so that most European manufacturers are able to provide these values reasonably easily. Although those simplified properties cannot reproduce anisotropic behavior, for many common fabric types, such as basket-weave single color patterns, this simplification does not lead to misclassifications [16,17] when the whole year glare protection performance is evaluated.

Given the need to provide guidance to designers, the European standard EN14501 [18] provides a glare classification based on fabrics' transmittance properties ($\tau_{v,\ n\text{-}n}$, $\tau_{v,\ n\text{-}diff}$ and cut-off angle), see "Table 7 – Glare control – Classification" of the EN14501. The classes refer to the expected effects of the fabrics: 0 for "very little effect", 1 for "little effect", 2 for "moderate effect", 3 for "good effect" and 4 for "very good effect". On the other hand, the European standard EN17037 [15] limits to 5% of a space's usage time the periods where DGP may exceed recommendations thresholds. The latter are: 0.35 for "high glare protection", 0.40 for "medium glare protection", and 0.45 for "low glare protection", which correspond to the glare protection categories associated with the DGP [13,19]. Combining the two, and depending on the geographical location of a given space (i.e., its "sunshine zone" defined in the EN17037), its orientation and the position of the desk in that space, classes of shading fabric (defined in the EN14501) can be associated to recommendations regarding protection against glare (see "Table E.6 – Recommended glare classes for fabric or non-fabric curtains according to EN 14501 to fulfil the glare criteria of $DGP_{e<5\%} \leq 0{,}35$" of the EN 17037).

Looking more closely at the these tables, we realize that only fabrics with low $\tau_{v,\ n\text{-}n}$ and low $\tau_{v,\ n\text{-}diff}$ would effectively be able to meet the criteria for adequate glare protection. Yet, it is important to remember that the DGP – which was used to define these thresholds – was developped in a set-up primarily using venetian blinds, not fabrics. Further, the recommended classes of the EN17037 were mainly based on a simulation study. The reliability of the thresholds for fabrics shadings thus remains open to question.

Recently, Yamin Garretón et al. [20] looked at the impact of fabrics properties on glare performance based on the DGP and found that fabrics with values of $\tau_{v,\ n\text{-}n} =< 0.03$ and $\tau_{v,\ n\text{-}diff} =< 0.03$ (i.e. within categories 3 and 4 of the EN 14501) could in fact offer a good protection against glare.

In their study questioning the applicability of glare metrics for shading fabrics, Konstantzos and Tzempelikos [21] found that the form of the DGP equation was actually adequate for fabric shading, but also that metrics based solely on the amount of light reaching the eye (e.g., Ev, DGPs) could not correctly characterize glare when the sun was in people's field of view [21]. They thus suggested an alteration of the DGP involving a change in the coefficients to make the model more suitable for predicting glare with shading fabrics. While this study offer a valuable contribution, the proposed model was not validated using independent datasets that were not used to develop the model. Addressing this gap, the present study undertakes two controlled laboratory investigations involving typical shading fabrics used for glare protection across different locations, with the aim of evaluating the applicability of both existing metrics and of standards recommendations.

2. Objectives

The objectives of this study are to:

(1) verify which discomfort glare metric would be the most adequate to characterize the visual comfort conditions obtained with shading fabric when the sun is in the field of view,
(2) assess the adequacy of discomfort glare classes of the EN17037 further defined in the EN14501.

For our first objective, we collected data via two human-subject experiments investigating discomfort glare with fabric shading with sun in the field of view, one in Lausanne, Switzerland and the other in Mendoza, Argentina. Both were conducted in semi-controlled office-like set-ups and relied on the following discomfort glare metrics: DGP, DGI, UGP and CGI to which a modified version of the DGP was added, which we will label DGP_{mod}, based on the findings from Konstantzos and Tzempelikos and the alterations they suggested to the DGP coefficients [21]. The equations pertaining to these metrics are reported in the appendices.

For our second objective, as experiments with human subjects, which can only be conducted at a defined date and moment for each participant (i.e. which relate to point-in-time situations), we had to resort to annual glare simulations to match the glare classification in the standard EN14501, which considers an annual behavior of the fabrics. To run these simulations, we relied on the measured optical behaviour of the fabrics using the same methodology as the one through which the classification tables for EN14501/EN17037 were derived.

3. Point-in-time user assessments

We used data from two tests on human subjects, one of which was carried out in Switzerland and the other in Argentina. Each study involved four shading fabrics, and we conducted our experiments for worst-case scenarios with low-sun position, i.e., so that each participant had the sun in their FOV behind the fabric when sitting at the desk. We used occupant surveys to capture their subjective perception, which we matched with measurements made with high quality instruments.

For a South-oriented space located in Lausanne, Switzerland (sunshine zone "L", i.e., with less than 2100 annual sunshine hours, in Northern hemisphere), with a large opening of glazing transmittance ($\tau_{v,\ n\text{-}h,\ glazing} = 0.79$), a viewing direction towards the façade and a distance to the façade varying between 1 and 2 meters, the recommended glare class according to the EN17037 is 4. Likewise, for a East-oriented space located in Mendoza, Argentina (sunshine zone "H", i.e., with at least 2100 annual sunshine hours, in Southern hemisphere), with a large opening of glazing transmittance ($\tau_{\ v,\ n\text{-}h,\ glazing} = 0.80$), a viewing direction towards the façade and a distance to the façade varying between 1 and 2 meters, the recommended glare class according to the EN17037 is 4. As such both experiments would be in need of the best performing fabric, i.e., with $\tau_{v,\ n\text{-}n} \leq 0.01$ and $\tau_{v,\ n\text{-}dif} \leq 0.03$.

3.1. Method

3.1.1. Fabrics properties

Our goal in selecting the fabrics was to focus exclusively on those capable of providing glare protection, while ensuring representation across the glare protection classes defined in EN 14501 (classes 1 to 4). We chose shading fabrics of different OFs and colors (gray and charcoal/black) and originally based the selection on the data provided by the manufacturers. We then also performed measurements using the scanning goniophotometers Model "pgII", Pab Advanced Technologies Ltd [22] from Realistic Graphics Lab (RGL), EPFL to derive $\tau_{v,n\text{-}h}$ and $\tau_{v,\ n\text{-}n}$. from the Bidirectional Transmittance Distribution Function (BTDF). We tested the diffraction of the black fabrics using a laser. Since we did not observe any diffraction, we considered OF equal to $\tau_{v,\ n\text{-}n}$ for the black fabrics and assumed the gray fabric (whose label begins with G) had the same OF as the black fabric from the same manufacturer and production series (whose label begins with B). This method is in accordance with EN14500:2021 Annex B1 [23]. All the values are reported in Table 1.

Table 1
Fabrics properties based on the manufacturer's data and on the measured data following two different measurement procedures.

Study	Fabric type	Color[b]	Measured data (goniophotometer)					Glare class
			$\tau_{v,\ n\text{-}n}$ (6°)	$\tau_{v,\ n\text{-}dif}$	$\tau_{v,\ n\text{-}h}$	Openness factor (OF)	Cut-off angle EN14500 (H / V)[c]	EN14501
AR	**B_1.1_AR**	Black	0.011	0.019	0.031	1.1%	**43**° (58°)	4
	B_4.0_AR	Black	0.040	0.019	0.059	4.0%	**55**° (61°)	1
	G_4.7_AR	Grey	0.047	0.023	0.069	4.0%	**55**° (61°)	1
	B_6.2_AR	Black	0.062	0.022	0.084	6.2%	**62**° (68°)	0
CH	**B_1.7_CH**	Black	0.017	0.002	0.019	1.7%	**50**° (62°)	4[d]
	B_2.3_CH[a]	Black	0.023	0.003	0.026	2.3%	61° (**69**°)	3
	G_3.7_CH	Grey	0.037	0.031	0.068	2.3%	**61**° (69°)	1
	B_6.1_CH	Black	0.061	0.007	0.068	6.1%	**62**° (69°)	0

[a] B_2.3_CH was positioned in the transversal direction because of the availability of the product for the desired width.
[b] The black fabric was labeled 'charcoal' in the manufacturer's documentation. However, we referred to it as 'black,' as the fabric was extremely dark, and this terminology aligns with the naming convention used for the fabrics ('G' for gray' and 'B' for 'black').
[c] The cut-off angle has been determined in the horizontal (H) and vertical (V) directions, using a 0.005 threshold for $\tau_{v,\ dir\text{-}dir}$ [EN14500]. Since B_2.3_CH was mounted in the transversal direction, we utlized the value of the vertical cut-off angle (bolded).
[d] According to the standard EN14501, the glare class moved up by one because of the low cut-off angle.
Acronyms: $\tau_{v,\ n\text{-}h}$ = Visible light transmittance normal-hemispherical (a.k.a., τ_v), $\tau_{v,\ n\text{-}n}$ = Visible light transmittance normal-normal, $\tau_{v,\ n\text{-}dif}$ = Visible light transmittance normal-diffuse

3.1.2. Experimental procedure

The procedure lasted about two hours and consisted of an introductory phase followed by five exposure sessions. Exposure sessions 1 to 4 were conducted with the shading fabrics fully down and presented in a randomized order, and a 5th session which was designed to study the user's behavior on the control of roller blinds. In this paper, we focus on sessions 1-4 and we focus on glare perception. A brief description of each facility is provided below:

(1) Lausanne Fabric Study (CH): a North-South oriented test unit (d*w*h = 6.55 m*3.05 m*2.65 m) with a large South-facing window (WWR 62%) located on the EPFL campus.
(2) Mendoza Fabric Study (AR): an East oriented test unit (d*w*h = 3.20 m*3.20 m*2.50 m) with an East-facing window (WWR 30%) located on the CCT CONICET campus in Mendoza.

The introductory phase involved the signing of consent form and the filling of a first background questionnaire. Only electric lights were used during the introductory phase. Each exposure session lasted about 12-15 minutes and involved a typing task and an exposure questionnaire. Daylight was the only source of light in the room during the experimental sessions. A typing task lasted about 5 minutes and was used to expose the participant to a typical office task before completing the survey. The exposure questionnaire followed the typing task. On average, participants needed about 5 minutes to complete the exposure questionnaire. Exposure sessions also involved a view clarity task which is not part of the present paper. There was a break of about 8 minutes between each session, which allowed the researchers to perform measurements, change fabrics and then repeat the measurements right before the next situation. Participants remained in the room during the break and were blindfolded.

For the Swiss study, 33 participants took part in experiments during the morning and early afternoon (9am-2:30pm) between December 2020 and March 2021 and again in October 2021. In Argentina, 24 participants took part in experiments carried out during the morning between October 2021 and November 2021. Photographs of the Swiss and Argentinian chambers are displayed in Fig. 1.

We excluded sessions with a variation of the outdoor global horizontal irradiance (GHI) greater than 25% measured each second by a pyranometer in both locations. Of the 33 participants from the Swiss study, we could keep partial data from 31 participants. The sun conditions were more stable in Argentina and all the data from the 24 participants could be kept.

3.1.3. Subjective measurements

The participants provided their personal information and subjective feedback about the environment by completing web-based questionnaires. The background questionnaire was used to collect baseline data from each participant (e.g., demographics, participant's mood, physical state at the time of the testing, etc.). The exposure questionnaires included comfort perception and preferences, and a set of visual comfort questions which were primarily about glare. We provided participants

Fig. 1. Photographs of the Swiss and Argentinian chambers during the testing.

with the definition of glare as "the sensation of visual discomfort caused by differences between light and dark areas, or by excessive brightness in your field of view" to minimize misunderstanding, and captured glare perception using different response scale assigned in random order. In this study, we focus on the binary, Osterhaus-Bailey and Likert (4 points) scales which are reported in Table 2. Each of these three scales has its own advantages and limitations, which are extensively discussed in the paper by Quek et al [24]. We chose them because they are commonly used in glare studies. The Swiss study used a questionnaire in English (as English is widely used on the EPFL campus), while the Argentinian study used a questionnaire translated into Spanish.

3.1.4. Glare measurements

In both studies, two LMT Pocket-Lux 2 hand-held illuminance sensors (class B certified to DIN 5032, part 7) were used: one of which was attached to the tripod right next to the luminance camera lens to measure Ev, and the other which could be positioned freely in the room (for example, on the participant's desk to measure desktop illuminance).

In the Swiss study, we also used a manufacturer calibrated luminance camera *LMK 98-4 color High-Resolution* camera with a "Dörr Digital Professional DHG" fish-eye lens (equidistant projection) and a neutral density filter ND4. The camera was was mounted on a tripod and manually positioned at the location of the participant and set to their eye level right before and right after each exposure to capture High Dynamic Range (HDR) images.

In the Argentinian study, we used a tripod-mounted Nikon D610 camera with a fisheye lens (Sigma 8 mm 1:3.5) instead, also combined to a neutral density filter ND4. Since the lens has an equid-solidangle projection, we applied a reprojection function to the equidistant image before applying vignette correction. The camera was manually positioned at the location of the participant and set to their eye level right after each exposure to capture HDR images. HDR generation was based on Pierson's tutorial [25], and the reference luminance values were obtained using a Minolta LS100 luminance meter.

We derived glare prediction models, namely DGP, CGI, UGP, and DGI, by running Evalglare version 3.02 [26,27] with default settings on the calibrated HDR images. DGP_{mod} was calculated based on the Evalglare output. We commonly used the HDR picture taken right after the exposure with the screen on, which we judged to be more representative. We utilized the images taken before the exposure only in the case of camera error for the image taken right after the exposure or sudden weather change.

3.1.5. Statistical analysis

We used descriptive statistics (mean and median values, the standard deviation, and the interquartile ranges) to report the overall visual conditions in the space by location, including occupants' responses for the derived glare metrics.

To derive the **glare thresholds**, we relied on Receiver Operating Characteristic (ROC) analyses, which discriminate between glare and non-glare situations. ROC curve illustrates the diagnostic ability of a binary classifier system as its discrimination threshold is varied. ROC analysis had been introduced to glare analysis by Rodriguez [28] and was also used to evaluate performance and robustness in a cross-validation study [4]. As ROC relies on binary classifier as input, only binary metric and metric converted to a binary format can be considered. The Osterhaus-Bailey scale was converted to binary with "disturbing" and "intolerable" considered as glare responses and the Likert scale was converted to binary with "moderately" and "very much" considered as glare response. ROC plots the "sensitivity" (aka. true positive rate) against "1 – specificity" (aka. false positive rate) and from this curve the ideal threshold can be determined following different methods. We used the average of the metrics "Youden" and "squared distance" on the R package "pROC". We looked at the whole sample as well as at the Argentinian and Swiss samples separately.

We then utilized two methods to determine the effectiveness of the glare metrics in **predicting** participant's subjective glare perception:

(1) The resulting area under the curve (AUC) from the ROC analysis is a prediction performance metric, with higher value corresponding to better prediction models. AUC output values range from 0 to 1 indicates the accuracy of a predictor where the diagonal line has an AUC of 0.5 and means random guessing. The closer a curve is to 1 (or 0), the more accurate a predictor is. We relied on Hosmer-Lemeshow et al. and on Safari et al. [29,30] for our interpretation of AUC value. AUC between 0.6 and 0.7 will be considered as poor classification accuracy, from 0.7 as acceptable classification accuracy and from 0.8 as excellent classification accuracy.

(2) The non-parametric Spearman's rank correlation test [31] measures the rank-based association between two variables. As such it helped determine the strength of the correlation between the glare metrics and participant's subjective perception. For this analysis, we used the R package "effsize". Binary metrics cannot be considered for this assessment and so we focused our analysis on the ordinal-scales (Osterhaus-Bailey, Likert). The strength of the correlation between two variables were determined by the Cohen's effect size thresholds [31] which were found to be in better agreement than Ferguson's more conservative thresholds [32] when compared to the ROC analysis and interpretations from the cross-validation study on glare measurements [4]. As such, we will consider a correlation coefficient $\rho > 0.3$ as a medium effect, and a correlation coefficient $\rho > 0.5$ as a strong effect. As the Spearman ρ obtained for the metrics varied, we further tested if this difference between the metrics was significant. For this analysis, we relied on a backtransformed average Fisher's Z procedure ("hittner2003" test [33]) for one-tailed alternative using the R package "cocor".

Table 2
Items from the exposure questionnaires we used to assess participants' perception of glare.

Name	Question	Response items
Binary	Are you experiencing any discomfort due to glare at the moment?	- Yes - No
Osterhaus-Bailey	At the moment, how would you describe glare in your field of view?	- Imperceptible - Noticeable - Disturbing - Intolerable
Likert (4pts)	How much discomfort due to glare are you experiencing at the moment?	- Not at all - Slightly - Moderately - Very Much

3.2. Results

3.2.1. Test conditions recording during the user assessments

A total of 220 data points was gathered by exposing 55 participants to four visual scenarios. However, after a strict verification of the weather conditions during the testing and a thorough examination of HDR images and vertical illuminance measurements of all the scenes, the final count of usable data points was of 191. These correspond to 99 data points from 31 participants from the Swiss study and 92 data points from 24 participants from the Argentinian study.

We derived five glare metrics (DGP, DGP_{mod}, DGI, UGP, CGI) by using Evalglare on the HDR images and relied on the measurements of the vertical illuminance (Ev) conducted during the testing. Fig. 2 shows the range E_v, DGP, DGP_{mod}, DGI, UGP and CGI by location and fabrics, and Table 3 provides additional statistical values on the same metrics and scenario. We note that the different fabrics combined with changes in time of day, day of year and weather conditions brought a nice spread

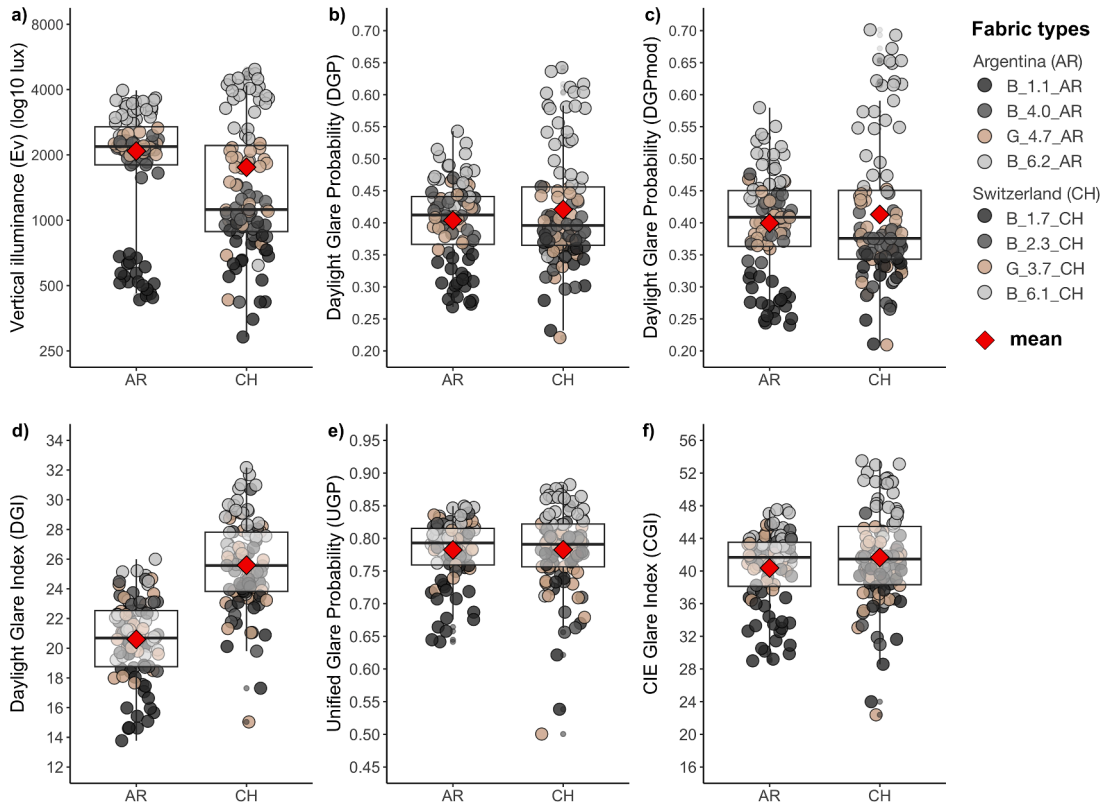

Fig. 2. Boxplot overlaid with a scatterplot showing the spread of glare measurements for 6 metrics: (a) vertical illuminance Ev, (b) Daylight Glare Probability (DGP), (c) modified Daylight Glare Probability (DGP_{mod}), (d) Daylight Glare Index (DGI), (e) Unified Glare Probability (UGP) and (f) CIE Glare Index (CGI), by location by location and fabric type.

Table 3
Descriptive statistics values for Ev, DGP, DGI, UGP and CGI by location and fabric types.

		Ev			DGP			DGPmod			DGI			CGI			UGP		
Loc.	**Fabrics**	**M**	**Mdn**	**SD**	**M**	**Mdn**	**SD**	**M**	**Mdn**	**SD**	**M**	**Mdn**	**SD**	**M**	**Mdn**	**SD**	**M**	**Mdn**	**SD**
All	*(all)*	1914	1940	1146	0.41	0.41	0.08	0.41	0.39	0.10	23.2	23.3	3.8	38	38.4	5	0.78	0.79	0.06
AR	*(all)*	2085	2185	965	0.40	0.41	0.06	0.40	0.41	0.08	20.6	20.7	2.8	37.8	38.4	4.2	0.78	0.79	0.05
CH	*(all)*	1720	1120	1277	0.42	0.39	0.09	0.41	0.38	0.11	25.6	25.6	3	38.3	38.4	5.6	0.78	0.79	0.07
AR	B_1.1_AR	545	520	85	0.31	0.31	0.03	0.28	0.28	0.03	17.1	16.9	2.2	31.8	32.1	3.0	0.71	0.72	0.04
	B_4.0_AR	2085	2120	244	0.41	0.42	0.03	0.41	0.41	0.03	21.6	22.3	2.0	39.5	40.1	2.3	0.80	0.81	0.02
	G_4.7_AR	2208	2185	175	0.41	0.41	0.03	0.40	0.40	0.03	21.0	20.7	1.9	38.3	37.9	2.7	0.79	0.79	0.03
	B_6.2_AR	3243	3270	337	0.47	0.47	0.03	0.49	0.49	0.04	22.1	21.9	2.1	40.6	40.5	2.4	0.81	0.81	0.02
CH	B_1.7_CH	694	707	208	0.36	0.37	0.04	0.33	0.34	0.04	24.0	24.2	2.5	35.3	36.7	4.6	0.75	0.77	0.06
	B_2.3_CH	1048	1050	217	0.38	0.39	0.04	0.36	0.36	0.04	24.9	25.1	2.5	37.2	38.5	4.3	0.77	0.79	0.05
	G_3.7_CH	1501	1620	524	0.39	0.39	0.05	0.38	0.38	0.06	24.7	24.8	2.9	35.8	36.3	4.6	0.76	0.77	0.06
	B_6.1_CH	3492	3750	1092	0.54	0.54	0.08	0.56	0.57	0.10	28.3	28.4	2.2	44.0	44.2	4.2	0.84	0.84	0.04

of the data for both locations. Overall, the Swiss results show wider spread than the argentinian data (especially in the higher range) which is reflected the higher standard deviations (SD). For the Argentinian data, E_v shows a gap between the least transmissive fabric (B_1.1_AR) and the others. This gap is likely caused by the large difference of the light transmittance (both $\tau_{v,\ n\text{-}n}$ and $\tau_{v,\ n\text{-}h}$) between B_1.1_AR and B_4.0_AR in combination with fewer changes in weather conditions in the Mendoza region, that has a continental, sunny and dry climate with a low cloud probability. We also note that mean E_v for the Argentinian sample is higher than for the Swiss sample, which means the experiments were conducted in higher adaptation levels in Argentina – an effect explained by differences in fabric properties and geographic location. DGI also showed large differences between the locations, with a substancial lower values for the Argentinian sample. The reason for this lies in a weakness of the DGI: in the denominator of its equation, the luminance of the glare source (multipled by the square root of the solid angle) is added to the background luminance without position correction and therefore the denominator gets significantly larger for the Argentinian data (since luminance is higher in this dataset). For DGP, DGP_{mod}, UGP and CGI, the large part of the output data, the mean and the median remains comparable across the two location, and either at the junction of the discomfort threshold (e.g., 0.40 for DGP and DGP_{mod}) or beyond (e.g., 22 for CGI and 0.5 for UGP).

Fig. 3 shows the sun positions seen from the participant's FOV, derived from the HDR images, overlaid with the Guth position index. In Argentina the sun positions as seen from the participant's FOV were substantially higher than in Switzerland (see Table 4), leading to higher position indexes ($P_{mean,\ AR}$=10.3, $P_{median,\ AR}$=10.1, $P_{,\ SD,\ AR}$=2.9 vs. $P_{mean,\ CH}$=3.5, $P_{median,\ CH}$=3.6, $P_{SD,\ CH}$=0.9, see also Fig. 3) which correlates with lower glare prediction. This difference in relative sun position (due to location and sun position) appear as the primary reason for the higher glare output observed in Switzerland.

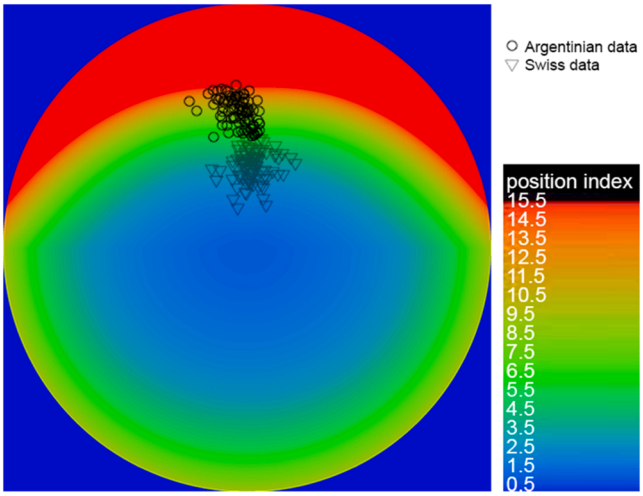

Fig. 3. Sun positions seen from the participant's FOV overlaid with the Guth position index, which is used in glare models.

Table 4
Descriptive statistics related to the sun position by location.

	Sun altitude				
	Min	**M**	**Mdn**	**Max**	**SD**
AR	42.0°	51.5°	51.7°	61.2°	5.3°
CH	15.3°	31.1°	31.7°	41.8°	5.6°

3.2.2. *Measured angular direct-direct transmittance*

Fig. 4 shows the results of the angular direct-direct transmittance measurements. The different angular transmittance behavior and the different sun positions per location and fabric-type can partly explain the differences in measured vertical illuminance and glare metrics (see Table 3). Remaining differences are likely caused by different azimuthal angles as well different sun intensities at the two locations. As result, fabrics B_1.1_AR and B_6.2_AR appear more protective in Argentina compared to fabrics B_1.7_CH and B_6.1_CH used in Switzerland, whereas B_2.3_CH and G_3.7_CH appear slightly more protective in Switzerland compared to B_4.0_AR and G_4.7_AR used in Argentina. Fabric properties and sun position explain these differences.

Another outcome of the angular measurements of the fabrics is the problematic of determining the "correct" cut-off angle for each fabric type. The method described in EN14500 (using the angle of incidence for $\tau_{v,\ dir\text{-}dir} = 0.005$) seems to be not appropriate especially for fabrics with $\tau_{v,\ n\text{-}n} < 0.03$ since it would shift the modelled direct transmittance curve for angles $> 45°$ to smaller values than in real. This is discussed more in detail in chapter 4.1.

3.2.3. *Participant's responses to glare exposure*

While the experimental conditions were originally planned to be comparable between locations, a careful assessment of the fabrics' properties using the goniophotometer showed substantial differences between them. In addition, the position of the sun was higher in Argentina leading to overall different conditions. Fig. 5 show the distribution of participants' responses for the different glare scales by location and by fabric. We observe that fabrics of class 4 (B_1.7_CH and B_1.1_AR) are rated best in terms of glare protection. However, B_2.3_CH (class 3) and G_3.7_CH (class 1) were rated similarly while the fabrics are categorized in different glare classes. The increase of overall brightness in the space due to the fabric color (gray for G_3.7_CH instead of black for B_2.3_CH) with much higher $\tau_{v,n\text{-}diff}$ has had a positive impact on glare perception due to the increase of the adaptation level. This effect does not appear as properly captured by the EN14501 classification scheme. A similar observation can be drawn for the Argentinian data, yet in this case the two fabrics belong to the same EN14501 glare class. In both locations, the fabrics of class 0 (B_6.1_CH and B_6.2_AR) show a poorly rated glare protection i.e. the glare class was assigned properly.

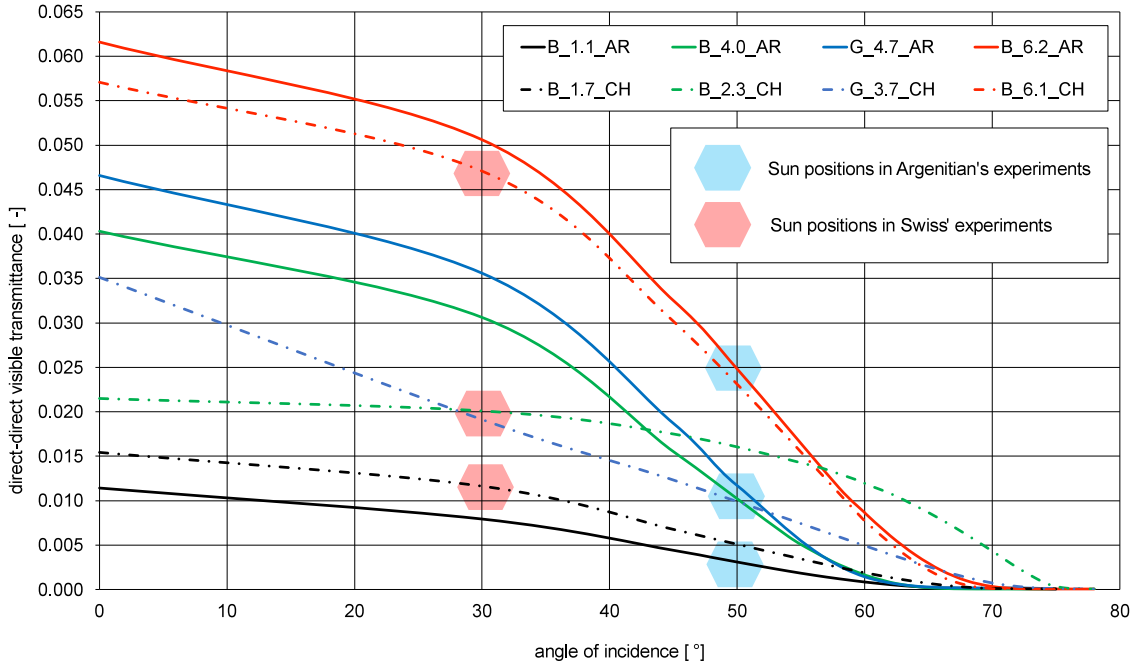

Fig. 4. Measured angular direct-direct transmittance $\tau_{v,\ dir\text{-}dir}$ for the different fabric types, derived from goniophotometer-measurements (6° integration angle around incident beam). Displayed values are for $\Phi = 0$ angle of the fabrics (except for B_2.3_CH ($\Phi = 90$) since mounted with a 90° rotation due to manufacturing constraints). While the Argentinian experiments were conducted in the rotating facility that was aligned perpendicular to the sun, the Swiss experiments were conducted in a fixed south-facing façade resulting in azimuthal angles between -54° and +34° (mean of -14°) towards the façade. This azimuthal difference results in different normal-normal transmittance values than displayed.

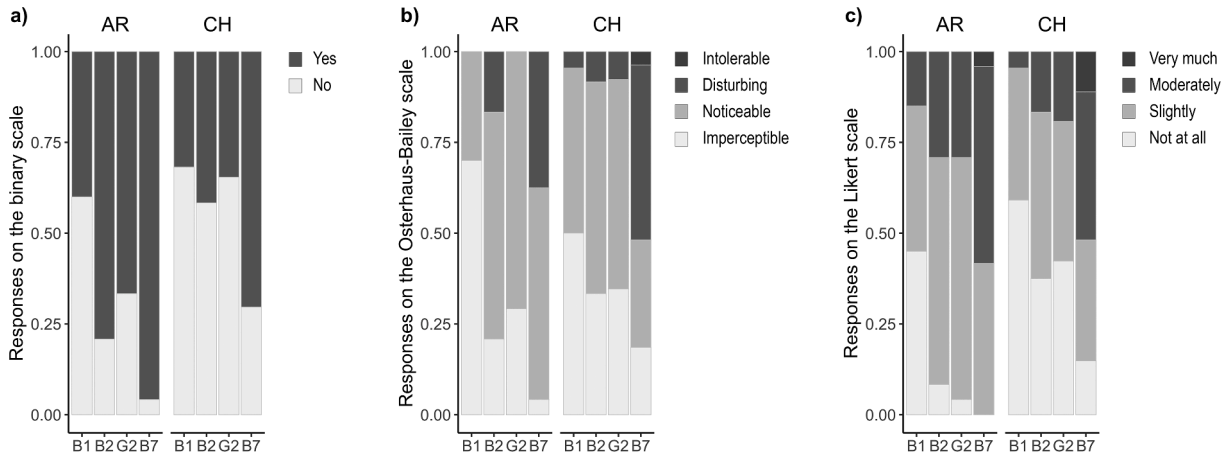

Fig. 5. Distribution of participants' responses for the different glare scales by location and fabric type (AR stands for Argentina, and CH stands for Switzerland).

3.2.4. Performance of daylight glare metrics prediction and glare thresholds

We conducted a ROC analysis to derive the AUC, one of the statistical measures to evaluate the performance of glare prediction metrics. We also used the ROC to determine glare thresholds for the underlaying experiments. As ROC is based on binary classifiers, we converted the ordinal scales to a binary format. As such, this analysis enables us to discriminate between instances of "no glare" vs. "glare", "noticeable" vs. "disturbing" glare and "slight discomfort" vs. "moderate discomfort" due to glare. We note that the numbers of participants having positively answered the questions is not the same following the different scales (see Table 5), which indicates different thresholds between the scales. Quek et al. found a similar behavior in a recent scale comparison study [24]. It should be noted here that the Argentinian study was carried out using a translated questionnaire and that the low response rate for "disturbing" on the Osterhaus-Bailey scale could also be due to languages subtleties. In fact, the translation of "disturbing" (the threshold chosen for discomfort glare) in "perturbador" may have been interpreted as something overly negative and so fewer people chose this option. This point suggests cultural variations linked to the languages in use in different regions.

The numeric results of the ROC analysis are reported in Table 6, and representative curves for all curves for the binary, Osterhaus-Bailey and Likert scales are shown in Fig. 6. Looking at the whole sample, we note that most metrics reached an AUC of 0.70 and that the highest AUC was obtained for the DGP (original and modified) using the Osterhaus-Bailey scale (AUC = 0.86). The DGI was overall the least performing metric. Looking at the Argentinian and Swiss sample separately, we note that the Swiss sample enabled higher prediction performance of the metrics, which is likely due to the larger variation in stimuli compared to the Argentinian experiments. In terms of thresholds, we see a trend for the binary scale generally leads to lower thresholds compared to the Osterhaus-Bailey. This result could be expected considering the results found in the scales comparison showing that the threshold of the binary scale lies between "noticeable" and "disturbing" on the Osterhaus-Bailey scale [24]. The thresholds found for the Likert lied in-between the binary and Osterhaus-Bailey scales. The thresholds for all metrics on the Osterhaus-bailey-scale are substantially higher than the ones calculated for the cross-validation study.

We used Spearman's rank correlation as a second measure to evaluate the effectiveness of glare metrics in predicting subjective responses. We applied it on the ordinal Osterhaus-Bailey and Likert glare scales of this study. The results are reported in Table 7. For the full sample all metrics show a Spearman ρ above 0.5 ($p<0.0001$) except for DGI, which means a strong effect size of the correlation between the metric and participant's responses for all the metrics. DGP overall showed the highest Spearman ρ. Looking at the Argentinian and Swiss sample separately, we note that the Swiss sample enabled higher prediction performance of the metrics, which is likely due to the larger variation in stimuli compared to the Argentinian experiments.

We tested if the difference between the Spearman ρ obtained between the different metrics was significant using the "hittner2003" test for one-tailed alternative. We conducted this analysis for the Osterhaus-Bailey response scale based on the full sample. The results are reported in Table 8. The test showed that DGI statistically differs to all the other metrics whereas the differences of correlation is not significant between DGP, $DGP_{mod,}$ CGI and UGP.

4. Simulation of the annual glare prediction to verify the glare classification

While experiments with subjects can be conducted only certain times throughout the year, the glare classification table in the standard EN14501 considers an annual behavior of the fabrics regarding discomfort glare and potential reflections on computer screens.

Table 5
Number of "positive" vs. "negative" votes for the full dataset as well as the Argentinian and Swiss dataset taken separately. "Positive" indicates that glare was detected, while "negative" indicates that participants did not report glare.

		Binary		Osterhaus-Bailey*		Likert*	
		Negative	Positive	Negative	Positive	Negative	Positive
All	count	80	111	159	32	136	55
	%	42%	58%	83%	17%	71%	29%
AR	count	26	66	79	13	61	31
	%	28%	72%	86%	14%	66%	34%
CH	count	54	45	80	19	75	24
	%	55%	45%	81%	19%	76%	24%

* The Osterhaus-Bailey and Likert scales were converted to binary format using the borderline between "noticeable" and "disturbing" glare and between "slight" vs. "moderate" discomfort due to glare, respectively.

Table 6
AUC for ROC and threshold (average of Youden and squared distance) for the daylight glare metrics with the considered glare scales. We bolded values for which AUC ROC ≥ 0.8 and marked in grey values for which AUC ROC < 0.6.

Scale*	Metrics	AUC ROC			Thresholds			
		Full sample	Argentinian data	Swiss data	Full sample	Argentinian data	Swiss data	Cross-validation study
Binary	**DGP**	0.76	0.78	**0.81**	0.41	0.41	0.39	-
	DGP_{mod}	0.77	0.78	**0.80**	0.39	0.41	0.38	-
	DGI	0.57	0.71	**0.80**	24.31	20.88	25.19	-
	UGP	0.76	0.75	**0.80**	0.78	0.80	0.78	-
	CGI	0.76	0.77	**0.81**	40.18	41.44	40.15	-
Osterhaus-Bailey	**DGP**	**0.86**	0.77	**0.91**	0.43	0.43	0.44	0.38
	DGP_{mod}	**0.86**	0.77	**0.91**	0.44	0.45	0.44	-
	DGI	0.74	0.65	**0.90**	26.25	20.15	27.37	19.9
	UGP	0.83	0.70	**0.91**	0.81	0.79	0.81	-
	CGI	0.84	0.71	**0.91**	42.21	41.44	43.88	31.0
Likert	**DGP**	0.74	0.64	**0.85**	0.41	0.42	0.41	-
	DGP_{mod}	0.75	0.65	**0.85**	0.42	0.43	0.39	-
	DGI	0.57	0.54	**0.82**	26.07	19.65	27.61	-
	UGP	0.69	0.56	**0.82**	0.80	0.79	0.81	-
	CGI	0.71	0.59	**0.84**	41.89	41.44	42.99	-

* The Osterhaus-Bailey and Likert scales were converted to binary format using the borderline between "noticeable" and "disturbing" glare and between "slight" vs. "moderate" discomfort due to glare, respectively.

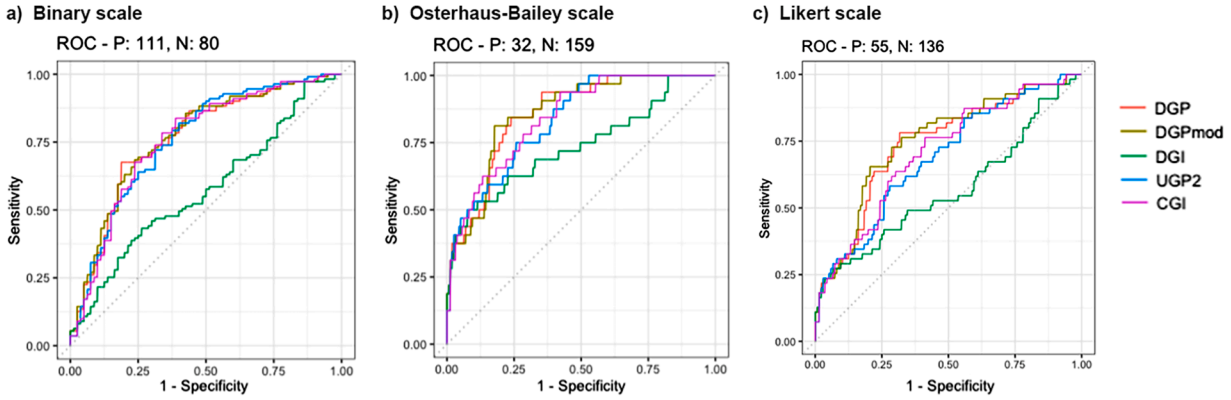

Fig. 6. ROC for the full sample on (a) the binary, (b) Osterhaus-Bailey and (c) the Likert scales, all converted to binary. The labels above the curves stands for count of positive (P) and negative (N) votes. The same values can be found on Table 5.

Table 7
Spearman ρ correlation between common daylight glare metrics and subjective responses on the Osterhaus scale.

Scale[(a)]	Metric	Full sample		Argentinian data		Swiss data	
		ρ	p-value[(a)]	ρ	p-value[(a)]	ρ	p-value[(a)]
Osterhaus-Bailey	**DGP**	0.57	<0.001	0.55	<0.001	0.59	<0.001
	DGP_{mod}	0.56	<0.001	0.56	<0.001	0.58	<0.001
	DGI	0.37	<0.001	0.43	<0.001	0.58	<0.001
	UGP	0.55	<0.001	0.48	<0.001	0.60	<0.001
	CGI	0.57	<0.001	0.51	<0.001	0.61	<0.001
Likert	**DGP**	0.51	<0.001	0.37	<0.001	0.61	<0.001
	DGP_{mod}	0.53	<0.001	0.38	<0.001	0.59	<0.001
	DGI	0.15	<0.001	0.22	0.04	0.59	<0.001
	UGP	0.46	<0.001	0.26	0.01	0.58	<0.001
	CGI	0.47	<0.001	0.29	<0.01	0.61	<0.001

[(a)] Significance levels: p<0.001 highly significant; p<0.01 significant; p<0.05 less significant.

Discomfort glare prediction in this standard is based on DGP and the occurrence of reflections on computer screens are considered by the vertical illuminance in display plane (see Table 9). In order to be able to relate the specific optical properties of the fabrics and the point-in-time evaluation of the experiments to a full year behavior, we conducted annual daylight simulations based on the methodology used to generate the tables of the EN14501.

4.1. Methods

This study replicates the simulation framework used to develop the EN14501 tables, incorporating similar modeling assumptions, climatic data, room and fabric geometries, and the exact properties of the fabric types tested in the user evaluation. Key methodological differences are:

1) how the shading configuration is treated: while the simulation model used to develop the tables of EN14501 assumes fully closed blinds

Table 8
Matrix reporting statistical significance (p-value and z) between the Spearman rank correlation obtained for the glare metrics on the Osterhaus-Bailey response scale using the full sample. If $p<0.05$ and $z > 1.96$ or < -1.96, the null hypothesis is rejected, meaning that the effectiveness of the metrics are statistically different.

Metrics	ρ	DGP_{mod} 0.5628	CGI 0.5656	UGP 0.5513	DGI 0.3662
DGP	**0.5701**	z = 1.14 p = 0.13	z = 0.36 p = 0.34	z = 0.92 p = 0.18	z = 3.70 **p < 0.001**
DGP_{mod}	**0.5628**		z = 0.16 p = 0.44	z = 0.47 p = 0.32	z = 3.31 **p < 0.001**
CGI	**0.5656**			z = 1.26 p = 0.10	z = 4.07 **p < 0.001**
UGP	**0.5513**				z = 3.64 **p < 0.001**

Table 9
Ranges of the 95th percentiles of DGP and monitor illuminances ($E_{v,M,95\%}$) used for the determination of the glare protection categories in EN14501.

	Glare protection category				
	Very good effect 4	**Good effect 3**	**Moderate Effect 2**	**Little effect 1**	**Very little effect 0**
$DGP_{95\%}$	≤ 0.30	0.30 < $DGP_{95\%}$ ≤ 0.35	0.35 < $DGP_{95\%}$ ≤ 0.4	0.4 < $DGP_{95\%}$ ≤ 0.45	> 0.45
$E_{v,M,95\%}$	≤ 1000 lux	1000 lux < $E_{v,M,95\%}$ ≤ 1500 lux	1500 lux < $E_{v,M,95\%}$ ≤ 2000 lux	1500 lux < $E_{v,M,95\%}$ ≤ 2000 lux	> 2500lux

that cover 100% of the window area, our approach allows for some daylight penetration by not lowering the blinds completely, thereby ensuring the minimum required light levels, that could be achieved in real world situations also by turning on the electric light. Applying this method avoids unrealistic low visual adaptation levels and therefore a potentially increased glare prediction, making this present simulation more aligned with real-world conditions.

2) how "eye blur" is accounted in the model: eye blur refers to the scattering effect within the human eye when the sun is visible in the field of view [34]. In this present study, eye blur is incorporated into the calculation of DGP, as it can significantly influence glare perception. For comparison purposes, we also computed DGP without accounting for eye blur, as this was the approach used in the simulations that informed the development of EN 17037 and EN 14501.

We used the material characteristics of the tested fabrics (see Table 1) in a simulation model. Both the model and the meteorological file of Frankfurt am Main (Germany) were identical to those used by Wienold et al. [35] and also those employed to draw up the tables in the standard. The weather file was extracted from the software Meteonorm [36]. The simulation model relies on Daysim to calculate the vertical illuminance and a successor method of the enhanced simplified DGP (eDGPs) method [6] that was validated in [37] to calculate DGP values in hourly timesteps.

The simulated room, visualized in Fig. 7, is 10 m wide, 5 m deep and 3 m high. It is South oriented. The reflectance values for the primary surfaces in the room are: 80% for the ceiling, 60% for the walls and 20% for the floor. All opaque surfaces are considered as purely diffuse reflecting. The window is made of a low-emissivity glazing ($\tau_{v,\ n\text{-}h}$ = 0.75) and the fabric blind starts at 1.25 and reaches 3 meter in height. To prevent overly dark situations which would artificially increase glare prediction due to the dominance of contrast in such situations, we used glass with a visual transmission of 20% (solar control glass) for the lower part of the facade (from the ground to 1.25 meter). This part of the façade is not covered by the fabric shade. The two calculation points are located at a distance of 2 meters from the façade, 1 meter from the side wall and at an eye height of 1.2 meters. The viewing direction is parallel to the façade. Points and directions are illustrated in Fig. 7 (right). For both points, we will calculate the annual 95th percentile DGP value (or $DGP_{95\%}$) between 8 and 18h. We will report only the higher value of the two (same approach than in [35]).

It should be noted that the participants' viewing direction are here parallel to the window, whereas in the user assessments (section 3), we wanted to maximize exposure to glare and thus the participant were facing the sun. A viewing direction parallel to the window is a more typical case and was therefore also used for the development of the classification tables in EN14501. The aim of the simulation study here is to apply the same annual evaluation method that was used for developing the EN14501 rather than reproducing the experimental cases.

We used the isotropic-cut-off simulation model [35] to describe the angular transmittance properties of the fabrics as this model was also used to develop tables in the EN14501 standard. First, we evaluated two simulation approaches: (1) the *standard model* and (2) the *adjusted model*. The standard model implements the procedure outlined in EN 14500 to determine the cutoff angle and employs the default p and q parameters of the underlying Roos model [38]. In contrast, the adjusted model refines both the cutoff angle and the p and q parameters through optimization, thereby achieving closer agreement with the measured angular transmission behavior (see Fig. 8). It is evident that the standard model shows significant deviations, particularly at low values of $\tau_{v,\ n\text{-}n}$. These discrepancies are primarily due to the procedure defined in EN 14500 for determining cut-off values, which relies on the angle of incidence at which $\tau_{v,\ dir\text{-}dir}$ equals 0.005. This fixed transmittance threshold is based on practical considerations related to measurement limitations and associated uncertainties. However, its application can obscure the real transmittance behavior, especially for materials with very low $\tau_{v,\ n\text{-}n}$ values. For instance, in the case of a fabric with an openness factor (OF) of 1% and a $\tau_{v,\ n\text{-}n}$ of 0.01, the threshold of 0.005 represents only half of the starting point of the transmittance curve and

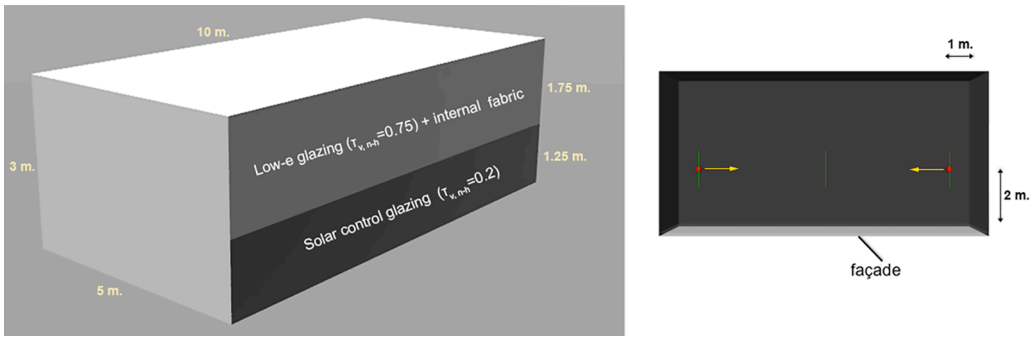

Fig. 7. Layout of the simulated room and position of calculation points (red dots: user's position, yellow direction: viewing direction).

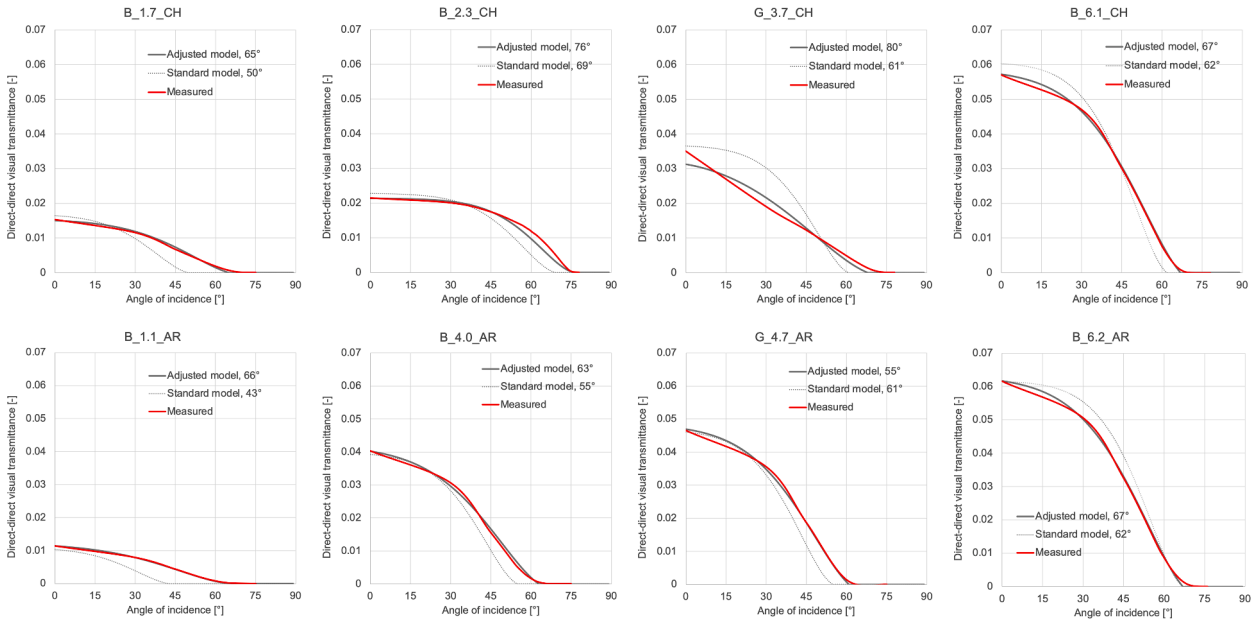

Fig. 8. Angular direct-direct visual transmittance behavior for the different fabric types and their isotropic simulation models (standard and adjusted). The measured data are derived for a rotation angle $\Phi = 0°$ (except for B_2.3_CH with $\Phi = 90°$ which was due to the mounting with a rotation of 90° due to production constraints). The standard model uses the cut-off-angle derived according to EN14500 using the incident angle resulting in a $\tau_{v,\ dir\text{-}dir}$=0.005 whereas the adjusted model uses an optimized cut-off angle, as well as optimized p and q parameters minimizing the difference between the modeled and measured transmittance curves.

misses a significant relative amount of light if we would built the integral of the transmittance curve and set the transmittance to zero for any value larger than that threshold. Consequently, this does not adequately reflect the intent of the cut-off—namely, to identify conditions of near-zero direct transmittance. Therefore, for future revisions of the standard, a revised methodology should be developed that not only accommodates measurement constraints but also more accurately characterizes the angular dependence of direct transmittance, which is the primary rationale for defining cut-off values.

4.2. Results

In this section we report the results of the simulations considering the eye blur and the usage of an adjusted fabric model on the annual glare behavior ($DGP_{95\%}$). We compared the individual classification using the simulation results to the tabular classification in EN14501 that is based only on $\tau_{v,\ n,n}$, $\tau_{v,\ n\text{-}dif}$ and the cut-off-angle. The results are summarized in Table 10.

These results show that using correct model-data, considering the eye blur-effect and a configuration leading to realistic adaptation levels is essential in the simulation otherwise a significant deviation of the glare prediction would occur. The main reason of the deviation between standard model and adjusted model is the value used for the cut-off angle. The method according to EN14500 turns out not appropriate to parametrize the simulation model, although the original intention was exactly that this value can be used as such. However, general limitations of measurement equipment led to the method to use the angle of incidence resulting in a $\tau_{v,\ dir\text{-}dir}$=0.005 as the cut-off angle (according to EN14500).

Adjusting only the 2-parameter standard isotropic simulation model to better fit the measurements would not change significantly the outcome (maximum absolute change of $DGP_{95\%}$ is 0.02) if the "right"

Table 10
Simulation results of the annual 95th percentile of hourly DGP value between 8 am to 6 pm (or $DGP_{95\%}$) and derived glare protection classes for the eight fabrics of this study.

Study	Fabric type	Measured data (goniophotometer)		Cut-off angle	Cut-off angle	Simulation $DGP_{95\%}$				Derived glare classes EN14501		
		$\tau_{v,\ n\text{-}n}$ (6°)	$\tau_{v,\ n\text{-}dif}$	EN14500	Derived optimized*	Standard model, cut-off: EN14500		Simulation adjusted model		Simulation adjusted model		Based on measured data
						without eye-blur	with eye-blur	without eye-blur	with eye-blur	without eye-blur	with eye-blur	
AR	**B_1.1_AR**	0.011	0.019	43°	66°	0.21	0.21	0.31	0.28	3	4	4
	B_4.0_AR	0.04	0.019	55°	63°	0.31	0.29	0.39	0.34	2	3	1
	G_4.7_AR	0.047	0.023	55°	61°	0.32	0.30	0.38	0.34	2	3	1
	B_6.2_AR	0.062	0.022	62°	67°	0.41	0.36	0.44	0.37	1	2	0
CH	**B_1.7_CH**	0.017	0.002	50°	65°	0.36	0.31	0.34	0.3	3	4	4
	B_2.3_CH	0.023	0.003	69°	76°	0.4	0.35	0.4	0.35	2	3	3
	G_3.7_CH	0.037	0.031	61°	80°	0.41	0.35	0.37	0.33	2	3	1
	B_6.1_CH	0.061	0.007	62°	67°	0.43	0.37	0.43	0.37	1	2	0

* The derived cut-off angles were determined by minimizing the difference between the measured and simulated direct-direct transmittance values, see Fig. 8. These values differ from those ones derived according to EN14500 using a transmittance threshold of 0.005.

Acronyms: $\tau_{v,\ n\text{-}n}$ = Visible light transmittance normal-normal, $\tau_{v,\ n\text{-}dif}$ = Visible light transmittance normal-diffuse

cut-off angle is provided, but could cause for extreme cases a switch of one class due to the absolute threshold classification scheme. Comparing the resulting classification of the adjusted model considering eye blur with the user assessment results one can observe a similar trend: 3 out of the 4 fabrics per location show good glare protection properties whilst the fabrics with OF>6% show a moderate performance. Comparing the (simplified) tabular classification of EN14501 with the (more detailed and accurate) simulation results reveals, that the tabular classification works reasonably well for lower $\tau_{v,\ n\text{-}n}$ values (< 3%), but underrates the glare protection potential for higher $\tau_{v,\ n\text{-}n}$ values or increasing diffuse transmittance values $\tau_{v,n\text{-}dif}$.

Lu et al. [16] recently conducted a simulation study suggesting optical properties of fabric shades depending on orientation and location and also compared their simulation findings to then EN14501 classification. However, their results are not directly comparable to those of our study. Similar to the methodology used to develop the EN14501 tables, Lu et al. assumed fully closed blinds, covering 100% of the window area. As noted earlier, this approach can lead to significantly low indoor illuminance, especially for low-transmittance fabrics, which can result in reduced visual adaptation and increased glare perception. Additionally, Lu et al. evaluated climates that differ from the Frankfurt climate used to develop the core classification table of EN14501 (Table 7), further limiting direct comparison.

5. Discussion

Daylight was the only source of illumination in the experimental session, as we aimed to avoid any potential influence from electric lighting. To maintain a minimum desk illuminance of 300 lux, we occasionally opened the curtains on the north façade (Swiss study) and the chamber's entrance door on the side facade. Although we considered raising the fabric shades to increase light levels, we ultimately decided against it, as the resulting view to the outside could have influenced participants' glare perception [39]. A similar concern regarding minimum illuminance levels and excessive contrast was taken into account in the simulation study, which led us to select solar control glazing for the lower part of the façade. While these design decisions may introduce some practical question, ensuring realistic illuminance levels was a key consideration in both studies.

The validation of the metrics revealed that DGP, DGP_{mod}, CGI and UGP performed well against user ratings with the fabrics tested (OF <7%), confirming the performance levels of the cross-validation study. By contrast, DGI performed less well and therefore cannot be recommended to be used to evaluate glare behind a fabric when the sun is visible through the shading. In general, the calculated thresholds in this study using DGP, DGP_{mod}, CGI and UGP are slightly higher than in the standards. These differences might be caused by the limited amount of fabrics and sun positions causing limited stimuli in this study compared to the much broader dataset used to derive the thresholds in the standards. However, all glare metrics sensitive to the way a glare source is extracted from the HDR image and a change in settings for the "peak extraction" that is responsible for the glare contribution from the sun-disk can change all metric values drastically. More research would be needed to reliably extract the glare sources from an HDR image to confidentially derive glare metrics and related thresholds is needed. The found slight overestimation of glare in this study indicates a too high threshold (i.e. a fixed value of 50 kcd/m^2) for the peak extraction in default glare source detection algorithm of Evalglare.

We observed no significant difference in performance between the original DGP and the modified version, DGP_{mod}. Furthermore, there was no noticeable trend favoring either version, indicating that they perform essentially the same.

Fabrics with $\tau_{v,\ n\text{-}n}$ <0.02 did not lead to much "disturbing" glare. On the other hand, the two fabrics with a $\tau_{v,\ n\text{-}n}$ around 0.06 caused a critical glare situation (e.g., "disturbing" and "intolerable") for 52% of the Swiss participants and for 38% of the Argentinian participants. The comparison of fabrics with an intermediate $\tau_{v,\ n\text{-}n}$ and OF, which we studied in black and grey colors (labelled as B_2.3_CH and G_3.7_CH (OF=2.3%) for Switzerland and B_4.0_AR and G_4.7_AR (OF=4%) for Argentina), shows that for each of the experiments carried out, the participants provided comparable subjective responses, although $\tau_{v,\ n\text{-}n}$ was much higher in the case of the brighter (grey) fabrics. This shows the importance to rely on metrics that are able to properly account for the adaptation level in glare prediction. Indeed, while the darker color of the fabrics implies a lower amount of light reaching the eye and therefore the level of adaptation is also lower leading to higher glare perception by the increased contrast. In a separate experimental session related to this present study, participants were allowed to operate the fabrics to their preferred position and most of them slightly opened the fabrics (on average by 25 cm between the window sill and the bottom of the blind) to bring more light in the room [40]. As such, increasing $\tau_{v,\ n\text{-}dif}$ does not necessarily increase glare.

The EN14501 tabular classification is a simplification that might end up in misclassification. The effect of increasing diffuse transmittance is well represented in the selected glare metrics but is too strongly considered in the tabular classification. As we only had one type of grey fabric in each study, we cannot conclude from these results at what values of diffuse transmittance the glare is perceived to be stronger (i.e., at what point the whole tissue becomes a source of glare and not just the visible sun disc). A classification based on $\tau_{v,\ n\text{-}n}$ and on $\tau_{v,\ n\text{-}dif}$ is always problematic for properties close to the considered thresholds. The simulation study revealed that for our data this classification using fixed bins of transmittance properties leads to an underrating of the glare protection properties compared to simulations using the measured optical properties. Overcoming this problematic may be achieved by replacing the table by an equation calculating a floating value for classification, based on $\tau_{v,\ n\text{-}n}$ and $\tau_{v,\ n\text{-}dif}$. Tests with higher $\tau_{v,\ n\text{-}n}$ (up to 0.1), as well for higher $\tau_{v,\ n\text{-}dif}$ (e.g., up to 0.15) could provide more data for the development of such an equation.

The simulation study also revealed that considering the eye blur and having realistic lighting levels is essential in glare simulations in order to avoid significant overestimation of glare. A limitation of the simulation study is its reliance on a simplified isotropic model for the fabric that uses only an angular beam transmittance in combination with ideal Lambertian scattering. In reality, the transmittance properties are anisotropic and forward-scattering in beam direction occurs, leading to a more complex BTDF than the model can represent and this might lead to differences in the glare calculation for specific fabric types, however the influence on annual values might be small [16,17].

Further, we found that the cut-off value was difficult to determine from the measurements. The transmittance value of 0.005 as threshold to determine the cut-off angle by the EN14500 turned out to be inappropriate to parametrize simulation models although it was originally intended. In general a better, reproduceable method is needed to describe the angular transmittance behavior of fabrics.

Lastly, when comparing glare classes derived from EN 14501, we observed notable differences between results based on measured data (to support our user assessments) and those from the simulation-adjusted model with eye blur. For example, B_6.2_AR and B_6.1_CH provided the least glare protection (class 0) with a window-facing view, while simulations with eye blur indicated a moderate effect (class 2) for a parallel view (see Table 10). This raises an important question: how should designers select roller shades? Our user study helped evaluate existing standards and glare metric thresholds, but they reflect only a moment in time. To address the frequency of glare events, we complemented the experiments with annual simulations, considering more typical desk positions, viewing directions and lighting levels resulting in realistic adaptation levels, and focusing on long-term performance rather than isolated critical conditions. We chose a parallel view in simulations as this was also used to develop Table 7 of the EN14501 standard and it aligns with best practice, and because designers are often unaware of future interior layouts determined by tenants. Ultimately,

one shall be aware that a key drawback of highly glare-protective fabrics is that they can significantly reduce daylight, potentially resulting in dim workspaces. For this reason, unless the space is used by light-sensitive individuals or involves critical viewing directions, we recommend a more balanced approach to fabric selection and to apply an adequate control for it considering besides glare aspects also daylight provision and view to the exterior.

6. Conclusion

This study compares subjective responses relating to discomfort due to glare from sunlight with calculated metrics based on measured daylight quantities. Data from two experiments conducted in Argentina and Switzerland were used to assess the applicability of glare metrics and their thresholds for situations with the sun visible through fabric shades, as well as on the recommendations of the standard EN14501 and EN17037.

User assessments indicate that fabrics with low normal-normal visual transmittance ($\tau_{v,\ n\text{-}n} < 0.05$) effectively prevent glare in critical situations (i.e., for low sun positions in the field of view). This outcome is also supported by the results of the simulations using the measured optical properties of the tested fabrics. For such simulations it is necessary to consider scattering effects of the eye causing blur otherwise the glare would be overestimated from the glare equations.

ROC analysis based on binary scales (or converted to binary) showed acceptable to excellent classification accuracy for DGP, DGP_{mod}, UGP and CGI. The related threshold of DGP for disturbing glare was calculated to 0.43, suggesting that using default glare source extraction in Evalglare in combination with the standard threshold of 0.40 slightly overestimates glare for shading fabrics. This needs to be investigated further by acquiring additional experimental data to extend the range of stimuli to be able to derive a more robust combination of glare source extraction method and related glare thresholds. The prediction performance based on the effect-size of the Spearman ρ correlation between the metric and participant's responses showed a strong correlation for DGP, DGP_{mod}, UGP and CGI when compared to subjective results on the Osterhaus-Bailey scale ($\rho > 0.5$). DGP provided the highest performance with a statistically significant difference to the performance of DGI, that cannot be recommended to be used for predicting glare when the sun disk is visible through shades. The metrics' performances of DGP_{mod}, UGP and CGI actually showed no significant difference to DGP. By comparing black and grey fabrics, we were also able to confirm that the level of adaptation of the metrics tested was adequately taken into account. While the amount-of-light-based measurements (E_v) showed very different values with this color change, the metrics of the study and the participants' subjective responses remained within a similar order of magnitude.

The tabular classification of EN14501 uses intervals of 0.01, which proves to be rather approximate, as in this transmittance range it is difficult to measure fabric properties reliably. As result, the standards may not be reliably applied. Further, by relying on five classes, the standard brings discontinuity in the classification of the fabrics and their assignation to geographic regions. Although a little less straightforward for practitioners, the use of equations and a numerical values (instead of a class) could enable more precise classification and recommendation by region. We also found that by recommending a glare class 4 (given the orientation, distance to façade and locations of our test chambers), the EN17037 appears quite conservative. Further, we found that the existing tabular classification is overestimating the glare from fabrics with higher normal-normal transmittance ($\tau_{v,\ n\text{-}n} > 0.03$) as well for fabrics with lighter colors (increasing $\tau_{v,\ n\text{-}dif}$).

CRediT authorship contribution statement

Caroline Karmann: Writing – review & editing, Writing – original draft, Visualization, Methodology, Investigation, Formal analysis, Conceptualization. **Jan Wienold:** Writing – review & editing, Visualization, Validation, Funding acquisition, Formal analysis, Conceptualization. **Julieta Alejandra Yamin Garreton:** Writing – review & editing, Methodology, Data curation. **Ayelén María Villalba:** Writing – review & editing, Methodology, Data curation. **Andrea Elvira Pattini:** Writing – review & editing, Funding acquisition. **Marilyne Andersen:** Writing – review & editing, Funding acquisition.

Declaration of competing interest

The authors declare that they have no known competing financial interests or personal relationships that could have appeared to influence the work reported in this paper.

Acknowledgments

This study is funded by Swiss National Foundation project (SNF) grant for the project "Visual comfort without borders: interactions on discomfort glare" number 200020_182151. This research was also supported by the National Scientific and Technical Research Council (CONICET) of Argentina, the National Agency for the Promotion of Science and Technology (ANPCYT) [grant numbers: PICT 2017-1088; PICT 2018-03269; PICT-2018-02080; PICT-2019-04356] and by the German Federal Ministry of Education and Research (BMBF) and the Baden-Württemberg Ministry of Science as part of the Excellence Strategy. We would like to thank Mermet SAS for their in-kind donation of the fabric blinds used in the Swiss experimental trials.

Appendix

Glare equations

Daylight Glare Index (DGI) [7,8]	$DGI = 10 \cdot log_{10} 0.48 \cdot \sum_{i=1}^{n} \left[\frac{L_s^{1.6} \cdot \Omega_s^{0.8}}{L_b + 0.07 \omega_s^{0.5} L_s} \right]$
Unified Glare Probability (UGP) [9]	$UGP = \frac{1}{\left(1 + \frac{2}{7} \cdot \left(10^{-\left(\frac{UGR+5}{40}\right)}\right)\right)^{10}}$
Unified Glare Rating (UGR) [10]	$UGR = 8 \cdot log_{10} \left(\frac{0.25}{L_b} \sum_{i=1}^{n} \frac{L_i^2 \cdot \omega_i}{P_i^2} \right)$
Daylight Glare Probability (DGP) [13]	$DGP = 5.87 \cdot 10^{-5} \cdot E_v + 9.18 \cdot 10^{-2} \cdot log_{10} \left(1 + \sum_{i=1}^{n} \frac{L_i^2 \cdot \omega_i}{E_v^{1.87} \cdot P_i^2} \right) + 0.16$

(continued on next page)

(*continued*)

Modified DGP (DGP_{mod}) [21]	$DGP_{mod} = 8.40{\cdot}10^{-5}{\cdot}E_v + 11.97{\cdot}10^{-2}{\cdot}log_{10}\left(1 + \sum_{i=1}^{n} \frac{L_i^2{\cdot}\omega_i}{E_v^{2.12}{\cdot}P_i^2}\right) + 0.16$
CIE Glare Index (CGI) [10,11]	$CGI = 8{\cdot}log_{10}\left(2{\cdot}\frac{1 + \frac{E_{dir}}{500}}{E_{dir} + E_{ind}}\right){\cdot}\sum_{i=1}^{n} \frac{L_i^2{\cdot}\omega_i}{P_i^2}$

With:
L_i Luminance of the i^{th} glare source
P_i Guth's position index of the i^{th} glare source
L_i Luminance of the i^{th} glare source
L_b Background luminance
L_{avg} Average luminance (E_v /π)
L_s Glare source luminance (cd/m2)
E_v Vertical illuminance at the eye (lux)
E_{dir} Direct illuminance from all glare sources
E_{ind} Indirect illuminance from field of view except glare sources
Ω_i Corrected solid angle of the i^{th} glare source weighted by position index ($d\omega_i$ / P_i^2)
ω_I Solid angle of the i^{th} glare source
ω_s Solid angle of a glare source (sr)

Nomenclature

$\tau_{v,\ n\text{-}dif}$ Visible light transmission normal-diffuse (en %)
$\tau_{v,\ n\text{-}n}$ Visible light transmission normal-normal (en %)
$\tau_{v,\ n\text{-}h}$ Visible light transmission normal-hemispherical (en %) (hemispherical = total)
$\tau_{v,\ dif\text{-}dir}$ Visible light transmission diffuse-direct (same as 'dif-n' for perpendicular light beam)
CGI CIE Glare Index
DGI Daylight Glare Index
DGP Daylight Glare Probability
DGP_{mod} Modified Daylight Glare Probability
FOV Field of view
UGP Unified Glare Probability
UGR Unified Glare Rating
WWR Window-to-wall ratio

Data availability

Data will be made available on request.

References

[1] CIE, CIE S 017:2020 ILV: International lighting vocabulary, 2nd edition, International Commission on Illumination, Vienna, Austria, 2020. https://cie.co.at/eilvterm/17-21-050.
[2] M.B. Aries, J.A. Veitch, G.R. Newsham, Windows, view, and office characteristics predict physical and psychological discomfort, J. Environ. Psychol. 30 (2010) 533–541.
[3] J.K. Day, B. Futrell, R. Cox, S.N. Ruiz, A. Amirazar, A.H. Zarrabi, M. Azarbayjani, Blinded by the light: occupant perceptions and visual comfort assessments of three dynamic daylight control systems and shading strategies, Build. Environ. 154 (2019) 107–121, https://doi.org/10.1016/j.buildenv.2019.02.037.
[4] J. Wienold, T. Iwata, M. Sarey Khanie, E. Erell, E. Kaftan, R.G. Rodriguez, J. A. Yamin Garreton, T. Tzempelikos, I. Konstantzos, J. Christoffersen, Cross-validation and robustness of daylight glare metrics, Light. Res. Technol. 51 (2019) 983–1013.
[5] CIE, CIE 252:2024 *assessment of discomfort glare from daylight in buildings, International Commission on Illumination*, Vienna, Austria, 2024. https://cie.co.at/publications/assessment-discomfort-glare-daylight-buildings.
[6] J. Wienold, Dynamic simulation of blind control strategies for visual comfort and energy balance analysis, in: Building Simulation, IBPSA Beijing, 2007: pp. 1197–1204.
[7] R.G. Hopkinson, Glare from daylighting in buildings, Appl. Ergon. 3 (1972) 206–215.
[8] P. Chauvel, J.B. Collins, R. Dogniaux, J. Longmore, Glare from windows: current views of the problem, Light. Res. Technol. 14 (1982) 31–46, https://doi.org/10.1177/096032718201400103.
[9] M.B. Hirning, G.L. Isoardi, V.R. Garcia-Hansen, Prediction of discomfort glare from windows under tropical skies, Build. Environ. 113 (2017) 107–120.
[10] CIE Technical Committee, CIE 117-1995 discomfort glare in interior lighting, International Commission on Illumination, Vienna, Austria, 1995.
[11] H. Einhorn, Discomfort glare: a formula to bridge differences, Light. Res. Technol. 11 (1979) 90–94.
[12] T. Iwata, M. Tokura, Examination of the limitations of predicted glare sensation vote (PGSV) as a glare index for a large source: towards a comprehensive development of discomfort glare evaluation, Int. J. Light. Res. Technol. 30 (1998) 81–88.
[13] J. Wienold, J. Christoffersen, Evaluation methods and development of a new glare prediction model for daylight environments with the use of CCD cameras, Energy Build. 38 (2006) 743–757, https://doi.org/10.1016/j.enbuild.2006.03.017.
[14] J.A. Jakubiec, C.F. Reinhart, The `adaptive zone'–A concept for assessing discomfort glare throughout daylit spaces, Light. Res. Technol. 44 (2012) 149–170.
[15] CEN, 17037, Daylight of Buildings, European Committee for Standardization, Brussels, Belgium, 2018.
[16] S. Lu, T. Wang, A. Tzempelikos, Glare-based selection of roller shade properties, Build. Environ. 265 (2024) 111954, https://doi.org/10.1016/j.buildenv.2024.111954.
[17] T. Wang, E.S. Lee, G.J. Ward, T. Yu, Field validation of isotropic analytical models for simulating fabric shades, Build. Environ. 236 (2023) 110223, https://doi.org/10.1016/j.buildenv.2023.110223.
[18] CEN, *EN 14501:2021 blinds and shutters - thermal and visual comfort - performance characteristics and classification, European Committee for Standardization*, Brussels, Belgium, 2021.
[19] C.F. Reinhart, J. Wienold, The daylighting dashboard – A simulation-based design analysis for daylit spaces, Build. Environ. 46 (2011) 386–396, https://doi.org/10.1016/j.buildenv.2010.08.001.
[20] J.Y. Garretón, A.M. Villalba, R.G. Rodriguez, A. Pattini, Roller blinds characterization assessing discomfort glare, view outside and useful daylight illuminance with the sun in the field of view, Sol. Energy 213 (2021) 91–101.
[21] I. Konstantzos, A. Tzempelikos, Daylight glare evaluation with the sun in the field of view through window shades, Build. Environ. 113 (2017) 65–77.
[22] Pab Advanced Technologies Ltd, Gonio-photometer pbII, (2022). http://www.pab.eu/?d=gonio-photometer (accessed May 5, 2022).

[23] CEN, EN14500:2021 Blinds and shutters – Thermal and visual comfort – Test and calculation methods, European Committee for Standardization, Brussels, Belgium, 2021.
[24] G. Quek, S. Jain, C. Karmann, C. Pierson, J. Wienold, M. Andersen, Comparison of questionnaire items for discomfort glare studies in daylit spaces, Light. Res. Technol. 55 (2023) 730–758, https://doi.org/10.1177/14771535231203564.
[25] C. Pierson, C. Cauwert, M. Bodart, J. Wienold, Tutorial: luminance maps for daylighting studies from high dynamic range photography, LEUKOS 17 (2020) 140–169, https://doi.org/10.1080/15502724.2019.1684319.
[26] J. Wienold, Evalglare–a new RADIANCE-based tool to evaluate daylight glare in office spaces, in: 2004.
[27] J. Wienold, M. Andersen, Evalglare 2.0–new features faster and more robust hdr-image evaluation, in: 2016.
[28] R.G. Rodriguez, J.A.Y. Garretón, A.E. Pattini, An epidemiological approach to daylight discomfort glare, Build. Environ. 113 (2017) 39–48.
[29] D.W. Hosmer Jr, S. Lemeshow, R.X. Sturdivant, Applied logistic regression, John Wiley & Sons, 2013.
[30] S. Safari, A. Baratloo, M. Elfil, A. Negida, Evidence based emergency medicine; part 5 receiver operating curve and area under the curve, Emergency 4 (2016) 111.
[31] J. Cohen, Statistical power analysis for the behavioral sciences, Lawrence Earlbaum Associates, Hillsdale, NJ, 1988.
[32] C.J. Ferguson, An effect size primer: a guide for clinicians and researchers, Prof. Psychol.: Res. Pract. 40 (2009) 532–538.
[33] J.B. Hittner, K. May, N.C. Silver, A Monte Carlo evaluation of tests for comparing dependent correlations, J. Gen. Psychol. 130 (2003) 149–168, https://doi.org/10.1080/00221300309601282.
[34] Transmittance thresholds of electrochromic glazing to achieve annual low-glare work environments, in: J. Wienold, S. Jain, M. Andersen (Eds.), Proceedings of the 10th BuildSim Nordic Conference, 2022, p. 8, https://doi.org/10.1051/e3sconf/202236208001. Copenhagen, Denmark.
[35] J. Wienold, T.E. Kuhn, J. Christoffersen, M. Andersen, Annual glare evaluation for fabrics, in: Proceedings of 33rd PLEA International Conference, 2017. Edinburgh, https://plea2017.net/#programmes-container.
[36] Meteotest AG, Meteonorm Software, (n.d.). https://meteonorm.com/en/ (accessed September 29, 2024).
[37] S. Wasilewski, J. Wienold, M. Andersen, A critical comparison of annual glare simulation methods, in: E3S Web of Conferences, EDP Sciences, 2022: p. 01002. https://www.e3s-conferences.org/articles/e3sconf/abs/2022/29/e3sconf_bsn2022_01002/e3sconf_bsn2022_01002.html (accessed June 26, 2024).
[38] A. Roos, P. Polato, P.A. Van Nijnatten, M.G. Hutchins, F. Olive, C. Anderson, Angular-dependent optical properties of low-e and solar control windows—: simulations versus measurements, Sol. Energy 69 (2001) 15–26, https://doi.org/10.1016/S0038-092X(01)00019-6.
[39] N. Tuaycharoen, The reduction of discomfort glare from windows by interesting views, University of Sheffield, 2006.
[40] C. Karmann, G. Chinazzo, A. Schüler, K. Manwani, J. Wienold, M. Andersen, User assessment of fabric shading devices with a low openness factor, Build. Environ. 228 (2023) 109707.